Submitted to the International Europhysics Conference on High Energy Physics,
HEP97, Jerusalem, Israel, August 1997

Measurement of the Diffractive Structure Function at Low Q^2

H1 Collaboration

Abstract

A measurement of the differential structure function $F_2^{D(3)}(\beta, Q^2, x_{I\!P})$ is presented in the kinematic region $0.8 \leq Q^2 \leq 5.0$ GeV^2, $0.01 \leq \beta \leq 0.4$ and $x_{I\!P} < 0.05$. When subjected to a Regge analysis, the data in this region require a dominant diffractive exchange together with additional contributions from a sub-leading exchange. In a fit to the new data together with previous measurements at larger Q^2, the diffractive trajectory is found to have intercept which is consistent with that determined using the previous measurements. Within the present experimental uncertainties, there is no evidence for any Q^2 dependence of the intercept $\alpha_{I\!P}(0)$ of the diffractive trajectory. Positive scaling violations of $F_2^{D(3)}(\beta, Q^2, x_{I\!P})$ at $x_{I\!P} = 0.005$ persist for $\beta \leq 0.4$ throughout the extended region of Q^2 covered by these data.

Abstract 377
Parallel Sessions 2,3,4
Plenary Sessions 1,2,3,4

1 Introduction

Using 1994 H1 data, the diffractive structure function $F_2^{D(3)}(\beta, Q^2, x_{I\!P})$, describing the process $ep \to eXY$ with[1] $M_Y < 1.6$ GeV and $|t| < 1.0$ GeV^2, has been determined in the region $4.5 \leq Q^2 \leq 75$ GeV^2 [1]. These measurements demonstrate that the dominant production mechanism at small $x_{I\!P}$ is diffractive. A non-diffractive contribution becomes increasingly important with rising $x_{I\!P}$ and falling β. The intercept $\alpha_{I\!P}(0)$ of the diffractive trajectory in a Regge motivated model has been found to be significantly larger than that [2] describing soft hadronic and photoproduction interactions.

During the 1994/95 HERA shutdown, the H1 detector was upgraded with a new electromagnetic and hadronic calorimeter (SPACAL) in the backward[2] region [3] and a new backward drift chamber system (BDC) in front of it. This new detector configuration extends the region of good acceptance to considerably lower Q^2 than has previously been possible.

In this paper, an analysis of H1 data taken in 1995 with the interaction vertex shifted by 70 cm in the proton beam direction is reported. The luminosity of the sample is 115 nb^{-1}. The data are used to make a first measurement of $F_2^{D(3)}$ at low $x_{I\!P}$ in the kinematic region $0.8 \leq Q^2 \leq 5.0$ GeV^2 and $0.01 \leq \beta \leq 0.4$, reducing the minimum value of Q^2 measured by a factor of 5 and the minimum β by a factor of 4. The data are used to perform a further study of the dynamics describing the differential structure function. In particular, the possibility of a Q^2 dependence of the diffractive trajectory and the Q^2 dependence of $F_2^{D(3)}$ at fixed $x_{I\!P}$ and β are investigated.

This paper should be read in conjunction with [1], which reports the measurements of $F_2^{D(3)}(\beta, Q^2, x_{I\!P})$ made with 1994 H1 data. The analysis techniques used in the two measurements are very similar and the cross section and kinematic variable definitions are identical. Only the changes with respect to the 1994 measurement are described in detail here. A full description of the present analysis can be found in [4].

2 Experimental Method

2.1 Event selection

The main trigger used in the analysis is based on an energy cluster in the SPACAL calorimeter, with full efficiency for electron energies $E'_e > 8$ GeV. Additional triggers with lower energy thresholds but limited statistics are also used to extend the analysis as far as $E'_e > 7$ GeV with trigger efficiency in excess of 99%.

The energy resolution of the SPACAL is $\sigma(E)/E = 7.5\%/\sqrt{E(\mathrm{GeV})} \oplus 2.5\%$ [3] and the spatial resolution of the BDC is better than 1 mrad. The electron energy is determined directly from the SPACAL energy measurement. The electron scattering angle is reconstructed from a BDC track together with the interaction vertex, determined from at least one central track. The selection criteria applied to isolate a sample of DIS events reflect the new detector configuration in the backward region and are summarized in table 1. The selection applied to the 1994 data with a shifted interaction vertex is also shown for comparison. In addition to these cuts, a further restriction $35 < \sum(E - p_z) < 80$ GeV is applied, where the sum extends over all final state hadrons and the scattered electron.

The selection of a sample of events containing large forward rapidity gaps has been tuned to the 1995 noise conditions. The selection is the same as that described in table 1b of [1] with the exception that the plug energy threshold is reduced from 5 GeV to 2.5 GeV and a further scintillator layer of the proton remnant tagger is used.

[1]The kinematic variables used to describe the analysis presented here are all defined in section 2 of [1].

[2]The backward direction is defined to be that of the electron beam.

	1995	1994
(1)	$E_e' > 7$ GeV	$E_e' > 10.5\,\mathrm{GeV}$
(2)	$Q^2 > 0.6\,\mathrm{GeV}^2$	$Q^2 > 3.5\,\mathrm{GeV}^2$
(3)	$160^\circ < \theta_e < 177.8^\circ$	$163^\circ < \theta_e < 176^\circ$
(4)	$\epsilon_1 < 3.2\,\mathrm{cm}$	$\epsilon_1 < 5.0\,\mathrm{cm}$
(5)	$\epsilon_2 < 2.0\,\mathrm{cm}$	$\epsilon_2 < 5.0\,\mathrm{cm}$
(6)	$\lvert z_{vtx} - z_{vtx}^0\rvert < 35\,\mathrm{cm}$	$\lvert z_{vtx} - z_{vtx}^0\rvert < 30\,\mathrm{cm}$

Table 1: Summary of event selection criteria used to isolate a sample of inclusive DIS events. The left hand column shows the cuts applied in the 1995 analysis. The right hand column shows the cuts applied in the 1994 analysis with the interaction vertex shifted by 70cm in the proton direction. Cuts 1-3 ensure that the scattered electron is in the acceptance region of the SPACAL and the BDC. Cuts 4 and 5 are electron identification estimators; ϵ_1 is the electron cluster radius, ϵ_2 is the smallest distance from the closest hit in the BDC to the electron cluster centre. Cut 6 requires a measured vertex within approximately 3σ of the nominal vertex position.

2.2 Kinematic Reconstruction

The inclusive DIS variables are reconstructed using the Σ method [5]

$$y_\Sigma = \frac{\Sigma}{\Sigma - E_e'(1-\cos\theta_e)} \qquad Q_\Sigma^2 = \frac{(E_e'^2 \sin^2\theta_e)}{(1-y_\Sigma)} \qquad x_\Sigma = \frac{Q_\Sigma^2}{s\ y_\Sigma}\ ,$$

where θ_e is the scattering angle of the electron relative to the proton beam direction, s is the squared ep centre of mass energy and $\Sigma = \sum(E - p_z)$ is the sum over all hadronic final state particles. The analysis has also been performed reconstructing these variables using the 'y - weighted average method' described in section 4.3 of [1]. The results are in good agreement with those presented here.

The mass M_X of the system X is reconstructed using the same energy flow algorithm that is described in [1, 6], such that calorimeter and tracking information is combined in a manner that avoids double counting. The invariant mass is then reconstructed according to $M_X = 1.15 \cdot [2yE_e(E+p_z) - p_T^2]^{1/2}$, where E, p_z and p_T are the reconstructed laboratory energy, longitudinal momentum and transverse momentum of all objects comprising X. The factor of 1.15 is applied to the reconstructed M_X to account for residual losses and is chosen to optimise the transverse momentum balance between the scattered electron and the final state hadrons.

An independent analysis has been performed reconstructing M_X using calorimeter information only and reconstructing y and Q^2 from the electron energy and scattering angle alone [7]. The results of the two analyses are in close agreement.

2.3 Cross Section Extraction

The cross section for the semi-inclusive process $ep \to eXY$ is measured, where the two hadronic systems X and Y are separated by the largest gap in the rapidity distribution of final state hadrons and Y is the system closest to the outgoing proton direction. As in [1], the results are corrected to the region $M_Y < 1.6$ GeV and $|t| < 1.0$ GeV^2. The intervals in β, Q^2 and $x_{I\!P}$ are chosen such that they are always larger than the resolution in each variable. All data points correspond to photon dissociation masses $M_X > 1.9$ GeV.

Corrections for detector inefficiencies and migrations of kinematic variables due to finite resolution are determined using the Monte Carlo simulation techniques described in section 3 of [1], with a full simulation of the H1 detector in its 1995 configuration. The diffractive structure function assumed in the simulation is identical to that used in [1], except for some reweighting in the region $Q^2 < 1.6$ GeV^2 to improve the description of the present data. Each data point is corrected to the bin centre using the parameterisation described in section 3.2. Radiative corrections are determined using the HERACLES program [8], interfaced to the RAPGAP event generator [9].

2.4 Error analysis

All systematic errors described in section 4.4 of [1] have been evaluated for this measurement. There is a 2% uncertainty in the SPACAL electromagnetic energy scale, a 1 mrad uncertainty in the electron scattering angle and a 20% uncertainty in the SPACAL hadronic energy scale. Together with the energy scale uncertainty of the liquid argon calorimeter and the scale uncertainty for track measurements, these represent the dominant contributions to the systematic errors.

3 Results

3.1 The differential structure function $F_2^{D(3)}(\beta, Q^2, x_{I\!P})$

In order to ensure that there are no uncontrolled systematic effects in the new data, $F_2^{D(3)}$ is determined in the large Q^2 regime of the 1994 measurement as well as the newly accessed low Q^2 region. A comparison of the 1994 and 1995 data in the form of the $x_{I\!P}$ dependence of $x_{I\!P} F_2^{D(3)}$ at various β and Q^2 values is shown in figure 4. In the overlap region, the two sets of data are in agreement to within the statistical errors on the 1995 data.

Figure 2 shows the 1995 measurements of $F_2^{D(3)}$ at lower Q^2. The measured differential structure function displays similar features to those of our earlier measurement at larger Q^2, with $x_{I\!P} F_2^{D(3)}$ either falling or flat as $x_{I\!P}$ increases throughout most of the kinematic region. There is evidence from these data alone for a change in the $x_{I\!P}$ dependence at the largest values of $x_{I\!P}$, with $x_{I\!P} F_2^{D(3)}$ rising most strongly in this region at small β.

3.2 Regge Phenomenological Parameterisation of the Data

The differential structure function measurements shown in figure 2 are used to further constrain the Regge phenomenological model developed in section 5 of [1], with parameters fixed in an identical way to that described in table 2 of that reference. A fit to the 1995 data only with a single trajectory of intercept $\alpha_{I\!P}(0)$, equivalent to fit A in section 5 of [1], does not give a good description of the data (χ^2/n.d.f. = 100.0/68 from statistical errors). Adding a second maximally interfering trajectory $\alpha_{I\!R}(t)$ with independent normalisation in each bin of β and Q^2 and performing a fit identical to fit C in [1] improves the description of the data considerably (χ^2/n.d.f. = 20.7/30). This confirms the conclusion from H1 data at larger Q^2 [1] and at $Q^2 = 0$ [6] that the semi-inclusive cross section with $x_{I\!P} < 0.05$ requires a substantial contribution from a sub-leading trajectory in addition to the diffractive mechanism.

A further fit of type C is performed in which the 1995 data are combined with the 1994 data points at $Q^2 \geq 7.5$ GeV^2. The fit results in an overall χ^2/n.d.f. = 154.9/154 and the value of $\alpha_{I\!P}(0)$ is almost identical to that obtained from the 1994 data alone. The results of this fit are superimposed on figure 2. There remains no sensitivity to the presence or absence of interference between the two trajectories.

The measurements described in [1] already establish that the intercept of the diffractive trajectory for $4.5 \leq Q^2 \leq 75$ GeV^2 is larger than that at $Q^2 = 0$, where the value obtained in a similar analysis is $\alpha_{I\!P}(0) = 1.068 \pm 0.016$ (stat.) ± 0.022 (syst.) ± 0.041 (model) [6]. To investigate whether there is any systematic variation in $\alpha_{I\!P}(0)$ within the measured DIS region, a further fit is performed to the combined 1994 and 1995 data with the pomeron intercept parameterised as $\alpha_{I\!P}(Q^2, t=0) = a_1' + a_2' \log(Q^2/10\,\mathrm{GeV}^2)$. The fit results in $\chi^2/\mathrm{n.d.f} = 155.3/153$ and a value for the Q^2 dependent term $a_2' = 0.012 \pm 0.016$ (stat.), consistent with zero to within statistical errors. The result excludes a fast variation of the intercept with Q^2 and is also consistent with $\lambda(Q^2)+1$ when the inclusive proton structure function is fitted to the form $F_2(x, Q^2) \propto x^{-\lambda(Q^2)}$ [10].

3.3 Scaling Violations of the Diffractive Structure Function

In [1], the β and Q^2 dependence of $F_2^{D(3)}(\beta, Q^2, x_{I\!P})$ was investigated at a fixed small value of $x_{I\!P}$ for which non-diffractive contributions are very small. Figure 3 shows the Q^2 dependence of the combined 1994 and 1995 results at $x_{I\!P} = 0.005$ in the region $\beta \leq 0.4$. The Regge fit to both sets of data with constant $\alpha_{I\!P}(0)$ is used to interpolate and extrapolate the data to this $x_{I\!P}$ value. It can be seen that throughout this region of β, scaling violations with positive $\partial F_2^{D(3)}/\partial \log Q^2$ persist throughout the newly accessed Q^2 range. This is in contrast to the case of the inclusive proton structure function $F_2(x, Q^2)$ [10], where $\partial F_2/\partial \log Q^2$ is approximately flat at $x = 0.15$. This result qualitatively confirms the conclusion that, if the diffractive exchange is describable in terms of parton distributions evolving according to the same QCD dynamics as those governing proton structure, the diffractive parton distributions at low Q^2 are dominated by gluons carrying large momentum fractions.

4 Summary

The diffractive structure function $F_2^{D(3)}(\beta, Q^2, x_{I\!P})$ has been measured in a new kinematic region at low Q^2. The qualitative features of the new data are consistent with those of previous measurements at larger Q^2. The $x_{I\!P}$ dependence at fixed β and Q^2 can be described by a combination of a diffractive and a sub-leading exchange. Including H1 data from both 1994 and 1995 in a Regge phenomenological fit, the leading singularity is found to have an intercept larger than that describing soft hadronic total, elastic and dissociation cross sections. Within the present experimental uncertainties, there is no evidence for any variation in the intercept of the diffractive trajectory in the region $0.8 \leq Q^2 \leq 75$ GeV^2. An investigation of the scaling violations of $F_2^{D(3)}(\beta, Q^2, x_{I\!P})$ at $x_{I\!P} = 0.005$ demonstrates for $\beta \leq 0.4$ that the rise at fixed β previously observed at large Q^2 persists throughout the newly accessed Q^2 range.

Acknowledgments

We are grateful to the HERA machine group whose outstanding efforts have made and continue to make this experiment possible. We thank the engineers and technicians for their work in constructing and now maintaining the H1 detector, our funding agencies for financial support, the DESY technical staff for continual assistance, and the DESY directorate for the hospitality which they extend to the non-DESY members of the collaboration.

References

[1] H1 Collaboration, C. Adloff *et al., Inclusive Measurement of Diffractive Deep-Inelastic ep Scattering*, paper submitted to this conference under abstract number 377, *idem* DESY **97-158**, to be submitted to Z. Phys. C.

[2] A. Donnachie, P. Landshoff, Phys. Lett. **B296** (1992) 227.
J. Cudell, K. Kang, S. Kim, Phys. Lett. **B395** (1997) 311.

[3] H1 SPACAL Group, R. Appuhn *et al.,* Nucl. Instr. and Meth. **A386** (1997) 397.

[4] M. Dirkmann, Ph. D. thesis (Univ. Dortmund), in litt.

[5] U. Bassler and G. Bernardi, Nucl. Instr. and Meth. **A361** (1995) 118.

[6] H1 Collaboration, C. Adloff *et al.,* Z. Phys. **C74** (1997) 221.

[7] T. Nicholls, *A Measurement of the Diffractive Proton Structure Function at HERA*, Ph.D. thesis (Univ. Birmingham), 1997 (unpublished).

[8] A. Kwiatkowski, H. Spiesberger, H. Möhring, Comp. Phys. Comm. **69** (1992) 155.

[9] H. Jung, Comp. Phys. Comm. **86** (1995) 147.

[10] H1 Collaboration, S. Aid *et al.,* Nucl. Phys. **B470** (1996) 3;
H1 Collaboration, C. Adloff *et al., A Measurement of the Proton Structure Function $F_2(x, Q^2)$ at low x and low Q^2 at HERA*, DESY **97-042**, submitted to Nucl. Phys. B.

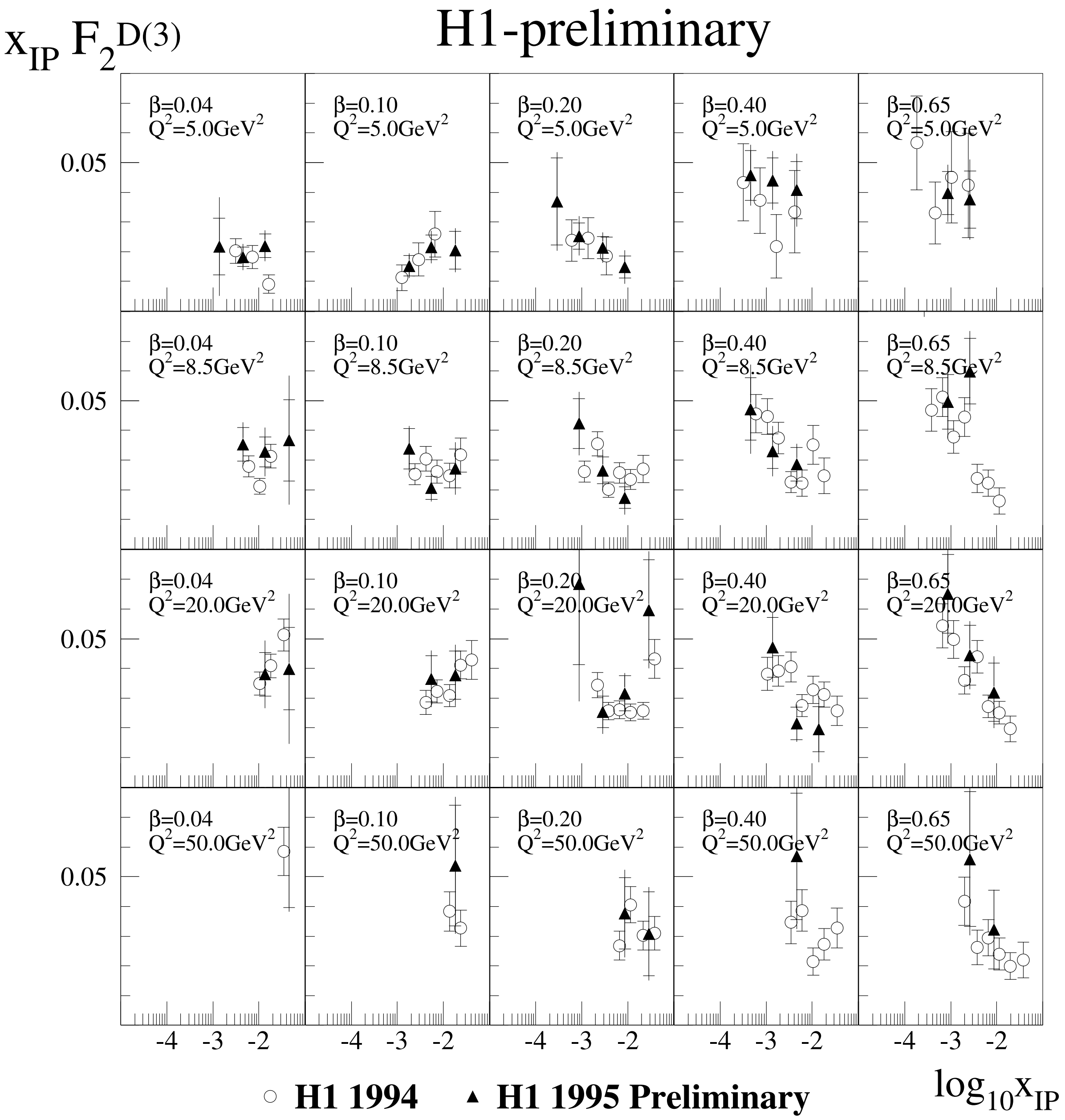

Figure 1: Comparison of 1994 and 1995 differential structure function measurements in the large Q^2 region. The quantity $x_{I\!P} F_2^{D(3)}(\beta, Q^2, x_{I\!P})$ is plotted against $x_{I\!P}$ for various β and Q^2 values. The inner error bars represent the statistical errors and the outer error bars the statistical and systematic errors added in quadrature.

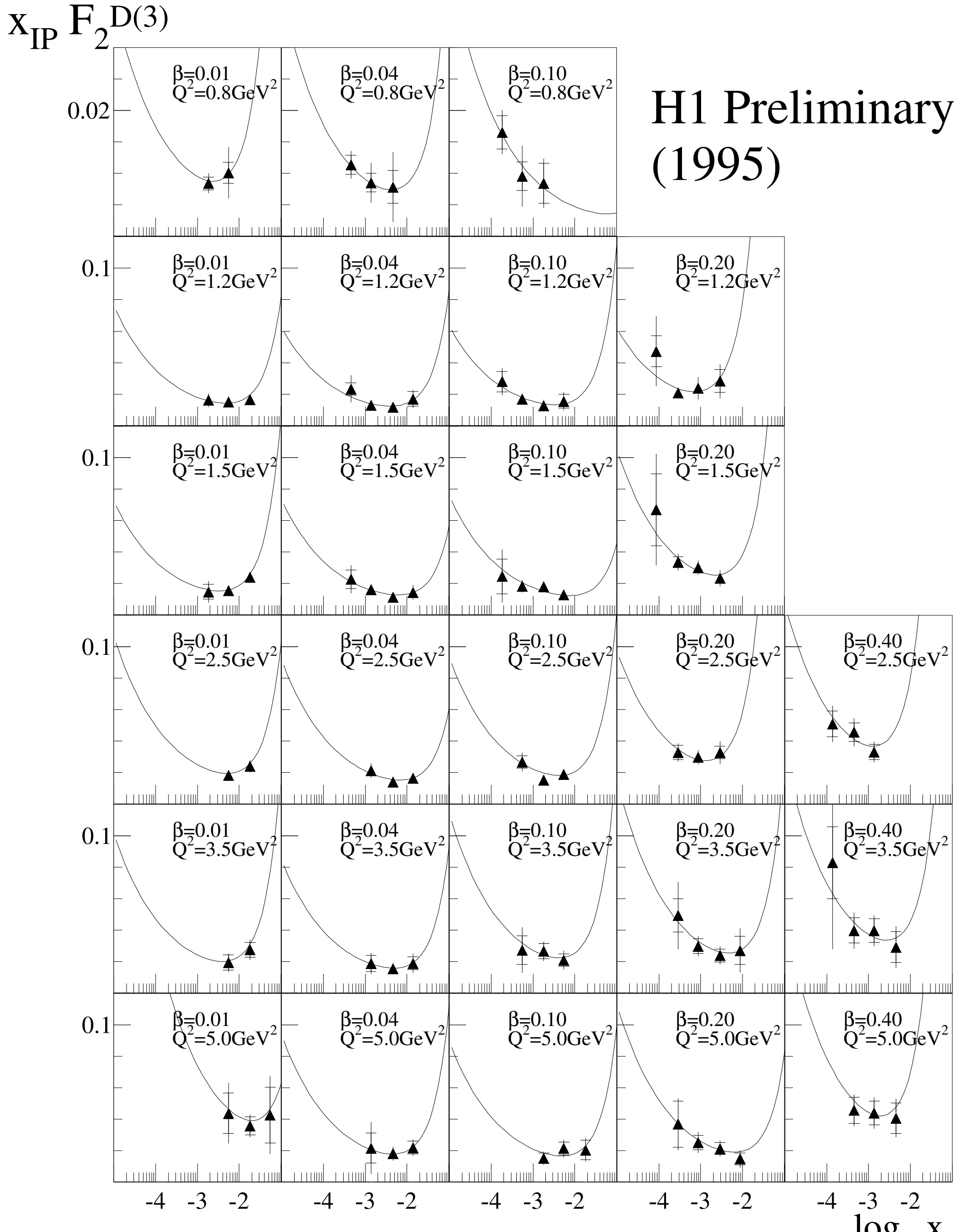

Figure 2: The differential structure function measured using 1995 data, plotted as $x_{\mathbb{P}} F_2^{D(3)}$ against $x_{\mathbb{P}}$ for various β and Q^2 values. The inner error bars represent the statistical errors and the outer error bars the statistical and systematic errors added in quadrature. The curves show the result of Regge fit C to the combined 1994 and 1995 data, with two fully interfering trajectories

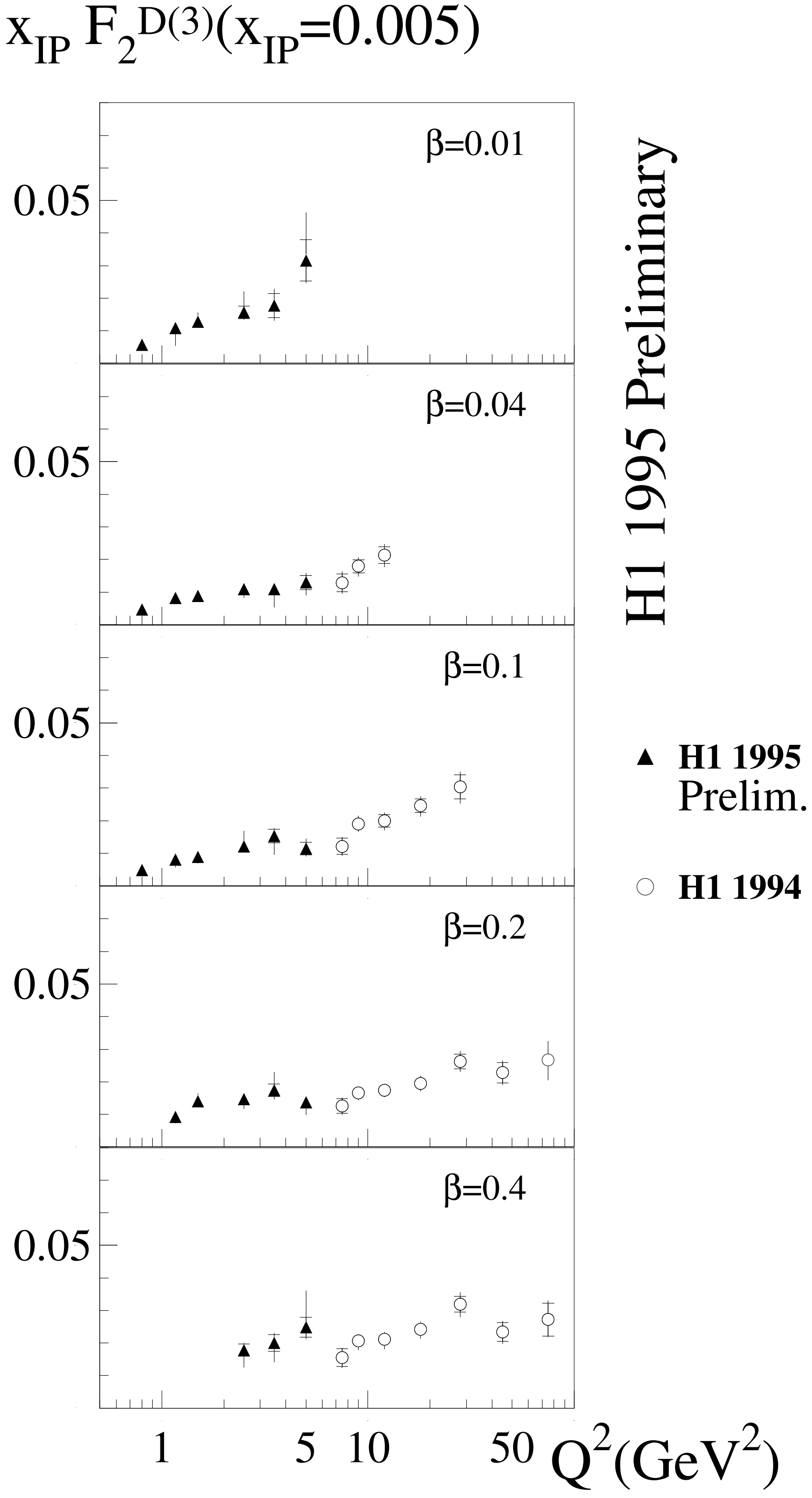

Figure 3: $F_2^{D(3)}(\beta, Q^2, x_{I\!P})$ at fixed $x_{I\!P} = 0.005$ as a function of Q^2 for various β values. Both 1994 and 1995 data are shown. The inner error bars represent the statistical errors and the outer error bars the statistical and systematic errors added in quadrature.